Development of a gene-activated scaffold platform for tissue engineering applications using chitosan-pDNA nanoparticles on collagen-based scaffolds.

AUTHOR(S)

Rosanne M. Raftery, Erica G. Tierney, Caroline M. Curtin, Sally-Ann Cryan, Fergal O'Brien

Title

Development of a Gene-Activated Scaffold Platform for Tissue Engineering Applications Using Chitosan-pDNA Nanoparticles on Collagen-Based Scaffolds

Authors

Rosanne M. Raftery[1,2,3], Erica G. Tierney[1,2,3], Caroline M. Curtin[1,2,3], Sally-Ann Cryan[1,2,4] and Fergal J. O'Brien[1,2,3*]

***Corresponding author**

F. J. O'Brien, Tissue Engineering Research Group, Department of Anatomy, Royal College of Surgeons in

Ireland, 123 St. Stephen's Green, Dublin 2, Ireland.

Tel: +353 (0)1 402 2149

Fax: +353 (0)1 402 2355

Email: fjobrien@rcsi.ie

Affiliations

[1] Tissue Engineering Research Group, Dept. of Anatomy, Royal College of Surgeons in Ireland, 123, St. Stephens Green, Dublin 2, Dublin, Ireland

[2] Trinity Centre for Bioengineering, Trinity College Dublin, Dublin 2, Dublin, Ireland

[3] Advanced Materials and Bioengineering Research Centre (AMBER), RCSI and TCD, Dublin, Ireland

[4] School of Pharmacy, Royal College of Surgeons in Ireland, 123, St. Stephens Green, Dublin 2, Dublin, Ireland

Abstract

Biomaterial scaffolds that support cell infiltration and tissue formation can also function as platforms for the delivery of therapeutics such as drugs, proteins and genes. As burst release of supraphysiological quantities of recombinant proteins can result in adverse side effects, the objective of this study was to explore the potential of a series of collagen-based scaffolds, developed in our laboratory, as gene-activated scaffold platforms with potential in a range of tissue engineering applications. The potential of chitosan, a biocompatible material derived from the shells of crustaceans, as a gene delivery vector was assessed using mesenchymal stem cells (MSCs). A transfection efficiency of >45% is reported which is similar to what is achieved with polyethyleneimine (PEI), a non-viral gold standard vector, without causing cytotoxic side effects. When the optimised chitosan nanoparticles were incorporated into a series of collagen-based scaffolds, sustained transgene expression from MSCs seeded on the scaffolds was maintained for up to 28 days and interestingly the composition of the scaffold had an effect on transfection efficiency. These results demonstrate that by simply varying the scaffold composition and the gene (or combinations thereof) chosen; the system has potential for a myriad of therapeutic applications.

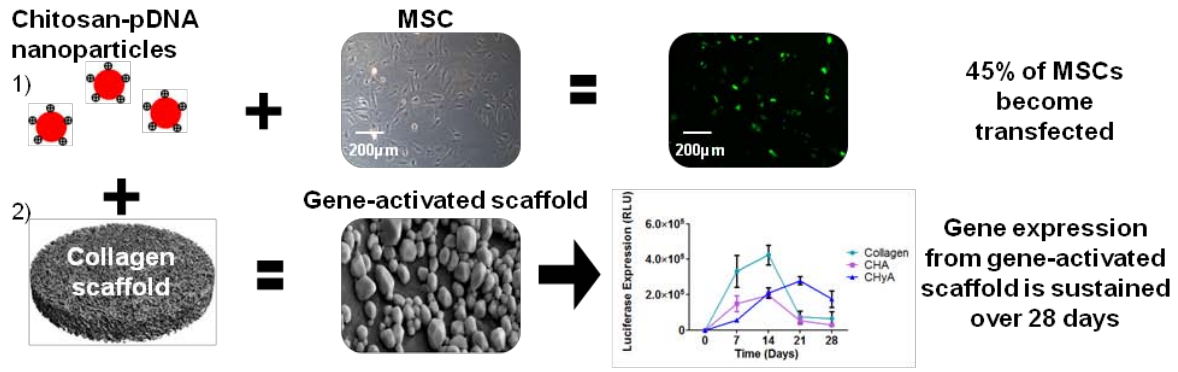

Table of Contents Graphic: Chitosan-pDNA nanoparticles combined with collagen scaffolds form a gene-activated scaffold platform for tissue engineering applications

Keywords

Chitosan nanoparticles, gene delivery, mesenchymal stem cells (MSCs), gene-activated scaffold, tissue engineering

1. Introduction

While the use of biomaterial scaffolds for the treatment of bone and cartilage defects has shown some promise, the addition of bioactive molecules such as growth factors can significantly enhance healing, particularly in large defects [1, 2]. For example, absorbable collagen sponges are used clinically to deliver recombinant human bone morphogenetic protein-2 (rhBMP-2) in spinal fusion procedures (Medtronic's INFUSE ®) [3]. However, as rhBMP-2 has a very short half-life, supraphysiological amounts of rhBMP-2 must be delivered in order to be effective. This can have adverse effects [4]. The delivery of genes-encoding growth factors, rather than the protein itself, offers a means of controlling the expression of protein at the defect site and prolonging the timeline of expression without needing repeated doses. Viral vectors are commonly used for gene therapy; however, there are many safety issues associated with their use such as immunogenicity and risk of insertational mutagenesis [5, 6]. On the other hand, non-viral gene delivery vectors have great potential in tissue engineering as they have a much better safety profile. However, non-viral vectors have not achieved the same levels of transgene expression (in a process termed transfection) as their viral counterparts, making vector design crucially important [7-10].

The ideal gene delivery vector must be biocompatible, biodegradable, minimally cytotoxic and capable of effective intracellular delivery of DNA [10]. It must also allow for sustained expression of the target protein for the required amount of time. Non-viral gene delivery vectors are typically formulated from two main groups of materials: 1) cationic lipids, for example, Lipofectamine 2000™, and 2) cationic polymers, for example, polyethyleneimine (PEI) [11-13]. However, both Lipofectamine 2000™ and PEI can be cytotoxic [14, 15] which has motivated research into more biocompatible materials.

Chitosan is a versatile biomaterial derived from the exoskeleton of many crustaceans which can be used in the formulation of microparticles and nanoparticles suitable for drug delivery [15-19]. The amine groups on the chitosan chain are positively charged and can bind to negatively charged DNA and condense it into positively charged nanoparticles. The use of chitosan for gene delivery is not a new concept, Mumper *et al.* (1995) first reported the use of chitosan for *in vitro* gene delivery 20 years ago [20]. However, to date the transfection efficiency reported using chitosan gene delivery vectors has been poor, especially in primary cells. Up to now, there have been only two reports detailing the

use of chitosan vectors to delivery genes to MSCs and the highest transfection efficiency reported was 18% [15, 21].

To facilitate endocytosis by cells and subsequent transfection, it is generally accepted that chitosan nanoparticles must be 100-200nm in diameter and carry an overall positive zeta potential (ZP) [15, 22]. Molecular weight (MW) is one of the main parameters affecting chitosan-mediated transfection as it influences nanoparticle size, complexation efficiency between chitosan and pDNA, rate and extent of endocytosis and eventual dissociation or 'unpacking' of the pDNA from chitosan [16, 23-25]. While high MW chitosan can form more stable nanoparticles, particularly when cross-linked, they may not release the pDNA efficiently thus limiting transfection. Conversely, low MW chitosan forms less stable complexes with pDNA but can result in more efficient release intracellularly [23]. Recently very low MW, water soluble oligochitosan (OCS: 7.3 kDa) has shown high transfection efficiency in a kidney cell line commonly used as a gene delivery model cell (HEK293 cells) [26]. This type of chitosan, which has not been used to transfect MSCs previously, was chosen for investigation as a non-viral vector in this study and compared to the more traditionally used polychitosan (PCS: 160 kDa) [15, 21].

The idea of combining therapeutic genes with biomaterial scaffolds was first proposed in the late 1990's and termed a 'gene-activated matrix' [27]. The theory is that when implanted *in vivo*, cells infiltrate the scaffold and internalise the gene delivery vector. The DNA is transcribed and translated to the target protein resulting in controlled release of the target protein at the site where it is required. Depending on the material composition of the scaffold, it might also support cell proliferation and differentiation and act to retain the genes at the defect site for longer, thereby delaying clearance. A series of porous collagen-based scaffolds, with the composition, pore structure and stiffness tailored to promote regeneration of individual tissues, have been developed for specific tissue engineering applications within our laboratory [28, 29]. Tissue healing induced by these scaffolds can be further enhanced by the incorporation of genes known to induce MSC osteogenesis or chondrogenesis and extracellular matrix deposition. PEI and nanohydroxyapatite (nHA) particles have been developed previously in our laboratory to deliver plasmids encoding bone morphogenetic protein-2 (pBMP-2) and vascular endothelial growth factor (pVEGF) on these collagen-based scaffolds and have resulted in almost complete repair of critical sized defects after just 4 weeks [30] post-implantation *in vivo*. However, as PEI can be cytotoxic and nHA is an osteoinductive biomaterial, a more biocompatible,

versatile delivery vector, namely chitosan, is required that could be used to create gene-activated matrices with potential use in a wide range of regenerative applications.

The objectives of this study was firstly, to develop chitosan-based nanoparticles with properties that facilitate MSC transfection and secondly, to create a series of gene-activated scaffolds by incorporating the optimised chitosan-pDNA nanoparticles into collagen-based scaffolds. Specifically, two types of chitosan were investigated as MSC transfection agents: a polymeric chitosan (PCS) of medium molecular weight (160 kDa) which has been used for MSC transfection and, while limited success was reported [15, 21], potential for gene delivery was shown. NovaFect™, an oligomeric chitosan (OCS) with a very low molecular weight (7.3 kDa) was also tested. This type of chitosan has not been tested on MSCs previously but has shown potential in cell lines such as HEK293 cells and cervical cancer (HeLa) cells as well as *in vivo* in corneal and retinal applications [26, 31, 32]. The optimal chitosan nanoparticle formulations were then applied to three different collagen-based scaffolds; collagen, collagen hydroxyapatite (CHA) and collagen hyaluronic acid (CHyA) which have previously been developed within our lab for repair of bone and cartilage [33-36] and the transfection efficiencies of the gene-activated scaffolds were determined.

2. Materials and Methods

All materials were supplied by Sigma Aldrich, Ireland unless otherwise stated.

2.1 Plasmid propagation

Plasmids encoding the genes *Gaussia* Luciferase (p*G*Luc; New England Biolabs, Massachusetts, USA) and green fluorescent protein (pGFP; Amaxa, Lonza, Cologne AG, Germany) under the control of the cytomegalovirus promoter were propagated by transforming One Shot® TOP10 Chemically Competent *E. coli* bacterial cells according to the manufacturer's protocol. pDNA was purified and collected using the Endotoxin free Maxi-prep kit (Qiagen, UK). Plasmid was dissolved in TE Buffer at a concentration of 0.5mg/mL and stored at -20^{o}C.

2.2 Chitosan-pDNA nanoparticle formulation

PCS (MW 160kDa; DD 85%) and OCS (Mw 7.3kDa; DD >97%) were supplied by Novamatrix, FMC Biopolymer, Norway. Nanoparticles were formulated by electrostatic interaction between cationic PCS

or OCS and anionic pDNA. Sodium tripolyphosphate (TPP) was used to further crosslink the PCS-pDNA particles. Nanoparticles were allowed to equilibrate for 30 min at room temperature before use. The ratio of chitosan to pDNA (N/P ratio) was varied as shown in Table 1. Branched PEI (MW 25 kDa) complexes were formulated as described previously [12] and used as a positive control in transfection experiments. Briefly, PEI was added to 2µg pDNA at an N/P ratio of 7. The formulation was mixed and allowed to complex for 30 mins at room temperature before use.

2.3 Physicochemical characterisation of chitosan-pDNA nanoparticles

2.3.1 Effect of MW on nanoparticle morphology

Nanoparticle size and morphology was determined using atomic force microscopy (Olympus IX51, Asylum Research MP3D, Gwyddion software) whereby, PCS-pDNA and OCS-pDNA nanoparticles were made as described in Section 2.2 and dropped onto a silicone substrate. Excess water was purged with nitrogen gas and samples were viewed immediately.

2.3.2 Effect of MW and N/P ratio on nanoparticle size and zeta potential and complexation efficiency

Dynamic light scattering (DLS) was also used to determine nanoparticle size and polydispersity and electrophoretic light scattering (ELS) was used to measure the zeta potential of the nanoparticles (Zetasizer 3000 HS, Malvern, UK). PCS-pDNA and OCS-pDNA nanoparticles were made as described above in Section 2.2 and the volume was brought up to 1 mL using molecular grade water and transferred to a zeta-cell (Malvern, UK) for analysis. Measurements were triplicated for three batches of nanoparticles and results are the average of three measurements. A SYBR® Safe (Life Technologies, Ireland) exclusion assay was used to assess how effectively OCS and PCS binds to pDNA. SYBR® Safe fluoresces strongly upon intercalation between the base pairs of pDNA and upon complete and stable binding of chitosan to pDNA there should be no free pDNA available for intercalation with the probe and the fluorescent signal is quenched [37, 38]. PCS-pDNA and OCS-pDNA nanoparticles were prepared as in Section 2.2 and then diluted to 1.5mL with molecular grade 20mM NaCl. 0.75µL of SYBRSafe DNA stain (Gibco, Ireland) was then added and the fluorescence signal read, in triplicate, on a spectrofluorimeter (Perkin Elmer LS 50B, Fisher Scientific, Ireland) at an excitation wavelength of 488nm and an emission wavelength of 522 nm.

2.3.3 Effect of MW and N/P ratio on nanoparticle stability

For efficient transfection, the vector must be capable of protecting the pDNA cargo from degradation *in vivo* by DNase enzymes. To examine the stability of chitosan-pDNA nanoparticles at both MW, PCS-pDNA and OCS-pDNA nanoparticles were made as described in Section 2.2 at a range of N/P ratios. $MgSO_4$ was added to give a final concentration of 0.1µM and the samples were incubated at 37^oC for 30 minutes with 8 units of DNase I per 1µg of DNA. Subsequently, 42µL of each sample was added to 6µL of 6X loading dye and 15µL of each was run on a 1% agarose gel for 1 hour, along with three controls; undigested nanoparticles, pDNA alone, and DNase-digested pDNA and a 1kB ladder. The gels were viewed under a UV transilluminator (Fisher Scientific, Ireland) and imaged using Syngene Genesnap technology (UK).

2.4 Development of an MSC transfection protocol using chitosan-pDNA nanoparticles

2.4.1 Stem cell isolation and expansion

Mesenchymal stem cells (MSCs) were isolated from 8 week old male Sprague Dawley rats with the approval of the Research Ethics Committee of the Royal College of Surgeons in Ireland (REC Approval No. 237). The MSCs were cultured in growth media which contained Dulbecco's Modified Eagles Medium supplemented with 2% penicillin/streptomycin, 1% L-glutamine, 10% FBS (Labtech, UK), 1% glutamax (Biosciences, Ireland) and 1% non-essential amino acids (Biosciences, Ireland). Cells were passaged at 70-90% confluency and expanded to passage 5 for all experiments. MSCs were seeded at a density of $5X10^4$ cells per well in 6 well adherent plates (Corning, Costar, Ireland) 24 h prior to transfection. Media was removed from cells 1 h prior to transfection and cells were washed in PBS. 1 mL of growth media was added to the PCS-pDNA groups and 1 mL of OptiMEM (Gibco, Ireland) was added to the OCS-pDNA groups. Nanoparticles were made as described in Section 2.2 and, following complexation, media was added in a 1:1 ratio to the nanoparticle mixture to produce the transfection medium of which 500 µL was added to each well. N/P ratio and pDNA dose were varied to determine the optimum conditions for transfection. After 4 h, transfection media was removed, cells were washed twice in PBS and growth media was replenished.

2.4.2 Effect of MW, N/P ratio and pDNA dose on MSC transgene expression

A reporter plasmid containing the gene for *Gaussia* Luciferase (pGLuc) was used in this study. The transfection efficiency of PCS-pGLuc nanoparticles formulated at N/P 10, 50, 100 and 150 and OCS-pGLuc nanoparticles made at N/P 10, 20, 30, 40, 50 and 60 were tested. The optimal pDNA dose was assessed by delivering 0.5, 1, 2 and 5µg/well. At pre-determined time points, samples of media were removed from the transfected cells and luciferase content was assessed using a Pierce™ *Gaussia* Luciferase Flash Assay kit (Thermo Scientific, Ireland) as per manufacturer's instructions.

2.4.3 Effect of MW on MSC transfection efficiency

The reporter plasmid containing the gene for green fluorescent protein (pGFP) was used in this study. PCS-pGFP nanoparticles were formulated at N/P 10 carrying 2µg of pGFP and OCS-pDNA nanoparticles were formulated at N/P 20 carrying 2µg of pGFP. At pre-determined time-points, fluorescent microscopy was also used to visualise cells expressing GFP using a Leica DMIL microscope (Leica Microsystems, Switzerland) and version 3.8 Leica software. The cells were then trypsinised and fixed in 5% formalin before being re-suspended in 200 µL of PBS. The suspension was then analysed for GFP fluorescence and a percentage of GFP positive over GFP negative cells gauged the transfection efficiency of the complex using FACS Canto 11 DIVA software.

2.4.4 Assessment of chitosan-pDNA nanoparticle toxicity

MSCs were transfected as described in Section 2.4.1 and an MTT Cell Growth assay kit (Millipore™, Ireland) was carried out at 1, 3 and 7 days post-transfection. This is a metabolic assay where active cellular enzymes reduce the MTT dye to formazan crystals. Briefly, 10 µL of MTT reagent was added to the cells in 90 µL of media and incubated for 4 h at 37°C. The supernatant was removed and 50 µL of dimethyl sulfoxide (DMSO) was added to dissolve the formazan crystals, formed by metabolically active cells, leaving behind a purple colour. The intensity of the resulting colour was read at an absorbance of 570 nm using a reference wavelength of 630 nm using a Varioskan Flash multimode plate reader (Fisher Scientific, Ireland).

2.5 Incorporation of chitosan-pDNA nanoparticles into collagen-based scaffolds to produce gene-activated scaffolds

2.5.1 Scaffold fabrication

Three different collagen-based scaffolds – collagen alone, collagen-hydroxyapatite (CHA) [35] and collagen-hyaluronic acid (CHyA) [36] were fabricated using a lyophilisation technique developed by O'Brien et al. [39]. The collagen slurry was made by adding 1.8 g of bovine tendon collagen (Integra Life Sciences, USA) to 360 mL of 0.5M glacial acetic acid (HOAc) and blending at 15,000 rpm for 90 mins using an overhead blender (Ultra Turrax T18 Overhead Blended, IKA Works Inc., USA) at a constant temperature of 4°C. The CHA scaffold was made using a patented protocol [28], briefly, 1.8g of bovine tendon collagen (Integra Life Sciences, USA) was added to 320mL of 0.5M HOAc and blended at 15,000rpm for 90 mins as described above. Two hundred wt%of hydroxyapatite (Captal 'R' Reactor Powder, Plasma Biotal, UK) was dissolved in 40 mL of 0.5M HOAc and added slowly to the collagen slurry (10mL/h) while maintaining dispersion at 15,000 rpm. After all hydroxyapatite has been added, the slurry was blended for a further 60 mins. The CHyA scaffold was made by blending 1.8g on bovine tendon collagen (Integra Life Sciences, USA) in 300mL of 0.5M HOAc for 90 mins. A total of 0.16g of hyaluronic acid sodium salt, derived from *streptococcus equi*, was dissolved in 60mL of 0.5M HOAc and added to the collagen slurry at a rate of 5mL/10 mins while blending at 15,000 rpm. The slurry was blended for a further 60 mins following the addition of all of the hyaluronic acid. Gas was removed from the slurries using a vacuum pump prior to freeze-drying (Advantage EL, Vis-Tir Co., Gardiner NY) to a final temperature of either -10°C (CHyA) or -40°C (Collagen and CHA) using a previously optimised freeze-drying profile [33]. The different freeze-drying temperatures used determine the resulting pore size with larger pores (~300µm) forming in scaffolds freeze-dried at -10°C compared to -40°C (~120µm) [40]. The scaffolds were crosslinked dehydrothermally (DHT) at 105 °C for 24 h at 0.05 bar in a vacuum oven (Vacucell 22; MMM, Germany) [41], followed by chemical cross-linking using a mixture of 6 mM N-(3-Dimethylaminopropyl)-N'-ethylcarbodiimide hydrochloride (EDC) and 5.5 mM N-Hydroxysuccinimide (NHS). Cylindrical scaffolds (10 mm diameter) were used in transfection experiments.

2.5.2 Gene-activated scaffold functionalization using optimised chitosan-pDNA nanoparticles

Scaffolds were manufactured as described in Section 2.5.1 and nanoparticles were made as described in Section 2.2. PCS-pDNA nanoparticles were formulated at an N/P ratio of 10 carrying 2 µg of while OCS-pDNA nanoparticles were formulated at an N/P ratio of 20 containing a 2 µg load of pDNA. Scaffolds were hydrated in PBS before use and nanoparticles were soak-loaded onto them by pipetting.

2.5.3 Assessment of gene-activated scaffold architecture

To visualise the nanoparticles on the scaffolds using SEM, 25 µL of the nanoparticle solution was added to each side of the scaffold. The samples were alcohol dehydrated in stages from 30%-50%-70%-90%-95%-100% alcohol leaving the samples for 30 minutes at each step. The samples were then placed on porous pots in a critical point dryer and the alcohol was slowly replaced with liquid CO_2. Once the alcohol was completely replaced, the pressure and temperature increased to the critical point for CO_2. At this point the liquid turns to gas and is vented off leaving dried samples. The samples were then mounted onto metallic studs using carbon cement before being sputtered with gold/palladium alloy and imaged using a Zeiss Ultra Plus scanning electron microscope (SEM) (Zeiss, Germany).

2.5.4 Measurement of transgene expression from MSCs seeded on gene-activated scaffolds

To assess the ability of chitosan nanoparticles to transfect MSCs on the collagen scaffolds, nanoparticles were made as described in Section 2.2. After complexation, 50 µL media containing $5X10^5$ cells were added to the nanoparticles and 50 µL of this was loaded onto each side of the scaffold. After 10 mins, 2mL of growth media was added. After 24h the scaffolds were moved to fresh 24 well non-adherent plates in fresh growth media. 3D transfections were performed with pGLuc and pGFP plasmids to quantify transgene expression on the scaffold. Samples of media were taken at days 7, 14, 21 and 28 and assessed for luciferase content using a Pierce™ Gaussia Luciferase Flash Assay kit (Thermo Scientific, Ireland). At the same time-points scaffolds with nanoparticles containing pGFP were imaged using a Leica DMIL microscope (Leica Microsystems, Switzerland) whereby GFP expression indicated positive transfection.

2.6 Statistical analysis

Results are expressed as mean ± standard deviation. In Figure 3 A-D, 4 D, 5 and 8 A and B, statistical significance was assessed using two-way ANOVA analysis followed by Bonferoni post-hoc analysis. The sample size was n=3 and $p \leq 0.05$ values were considered statistically significant where * $p<0.05$, ** $p<0.01$ and *** $p<0.001$.

3. Results

3.1 Physicochemical characterisation of chitosan-pDNA nanoparticles

3.1.1 Effect of MW on nanoparticle morphology

Nanoparticle morphology was visualized using Atomic Force Microscopy (Figure 1A and 1B). These images showed that the cross-linked PCS forms consistent homogeneous nanoparticles when complexed with pDNA (Figure 1A) and have an average diameter of 188.3 ± 16.5 nm while the OCS-pDNA nanoparticles have a much less defined structure, appearing like toroid and rod shaped complexes (Figure 1B). The OCS-pDNA nanoparticles also have a smaller diameter with an average of 119.9 ± 22.9 nm.

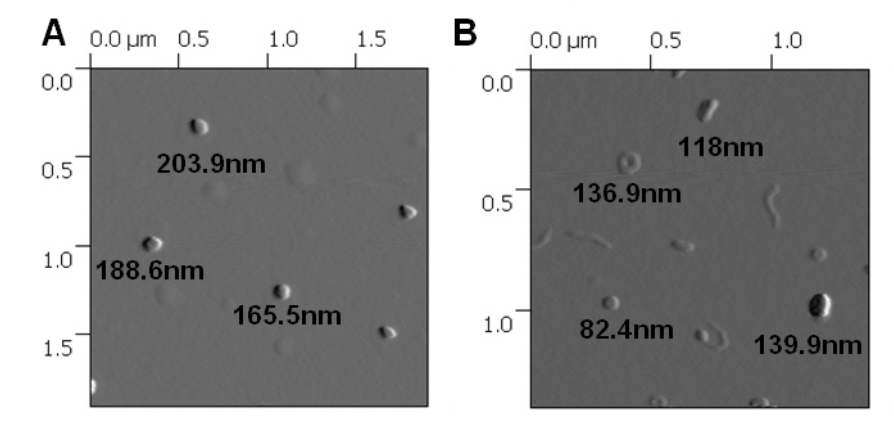

Figure 1: Effect of MW on chitosan-pDNA nanoparticle morphology. Representative AFM images of PCS-pDNA (A) and OCS-pDNA (B) nanoparticles. Average size of PCS-pDNA nanoparticles at N/P 10 was 188.3 ± 16.48 and OCS-pDNA nanoparticles at N/P 20 was 119.96 ± 22.94 which was in agreement with DLS measurements shown in Table 1.

3.1.2 Effect of MW and N/P ratio on nanoparticle size, zeta potential and complexation efficiency

Nanoparticles were also analysed for size as well as zeta potential using a Zetasizer 3000 HS (Malvern, UK) . PCS-pDNA nanoparticles formulated at N/P 10, 50, 100 and 150 met the size

(<200nm), zeta potential (+) and complexation criteria while at N/P 1 the nanoparticles were >200nm, negatively charged and did not encapsulate the pDNA sufficiently (70%) (Table 1) and at N/P ratios higher than 150, the nanoparticles were >200nm (Table 1) which may prevent cell uptake [42, 43]. Overall, the OCS-pDNA nanoparticles were smaller than the PCS-pDNA nanoparticles with an average diameter of 95.6 nm for OCS compared to 247.9 nm for PCS, a result which was expected due to the shorter length of the OCS chain [26]. The zeta potential of the OCS-pDNA nanoparticles did not vary much with increasing N/P ratio; however, the PCS-pDNA nanoparticle ZP ranged from -6.52mV up to +52.7mV. A SYBR®Safe exclusion assay was employed to demonstrate the complexation efficiency between chitosan and pDNA shown in Table 1. OCS form complexes with pDNA with a higher encapsulation efficiency (average of 93.5%) than PCS (average of 84.5%).

Table 1. Physicochemical characterisation of PCS-pDNA and OCS-pDNA nanoparticles.

Type of Chitosan	N/P Ratio[a)]	Size (nm)[b)]	Polydispersity Index[b)]	Zeta Potential (mV)[b)]	Encapsulation Efficiency (%)[c)]
PCS	1	295.03 ± 1.40	0.220	-6.52 ± 5.72	70.97 ± 2.57
	10	191.67 ± 7.49	0.250	26.67 ± 1.05	88.77 ± 0.60
	50	137.80 ± 42.29	0.247	48.30 ± 0.44	86.57 ± 0.24
	100	109.40 ± 10.15	0.252	49.30 ± 1.75	87.28 ± 0.15
	150	143.30 ± 16.46	0.290	52.70 ± 2.23	85.17 ± 0.45
	200	248.92 ± 16.34	0.359	48.43 ± 1.25	86.50 ± 0.33
	300	609.13 ± 13.73	0.208	51.03 ± 0.84	96.74 ± 0.37
OCS	10	98.63 ± 16.28	0.296	34.50 ± 3.66	92.80 ± 0.21
	20	109.26 ± 16.82	0.252	33.50 ± 2.60	93.57 ± 0.02
	30	76.87 ± 1.47	0.256	27.63 ± 0.59	93.36 ± 0.27
	40	125.87 ± 13.27	0.294	26.70 ± 2.55	94.80 ± 0.07
	50	73.70 ± 3.55	0.217	27.23 ± 3.59	93.71 ± 0.06
	60	89.46 ± 8.57	0.276	26.73 ± 5.68	92.60 ± 0.11

[a)] Nanoparticles were formulated at these N/P ratios carrying 2µg of pDNA
[b)] Size, polydispersity and zeta potential were assessed using a Malvern Zeta Sizer Nano Series 3000
[c)] Encapsulation efficiency was determined using a SYBRSafe exclusion assay

3.1.3 Effect of MW and N/P ratio on nanoparticle stability

The gels in Figure 2A and 2B compare pDNA complexed with both types of chitosan to naked pDNA and undigested chitosan nanoparticle controls. Exposure to DNase I for just 30 minutes completely destroys the naked pDNA as evidenced by the lack of fluorescence from that well, while the pDNA that was complexed with PCS and OCS remains intact. In the PCS-pDNA gel, there appears to be less pDNA at higher N/P ratios which indicates complete encapsulation at these ratios with a significant excess PCS compared to pDNA. No banding is seen on the gel in the PCS-pDNA group

(Figure 2A) which indicates that the pDNA is still strongly encapsulated by the PCS after DNase I treatment, however, in Figure 2B, evidence of faint bands can be seen at all N/P ratios in the OCS-pDNA group, but more so at lower N/P ratios, which suggests that the pDNA is beginning to be released from the OCS.

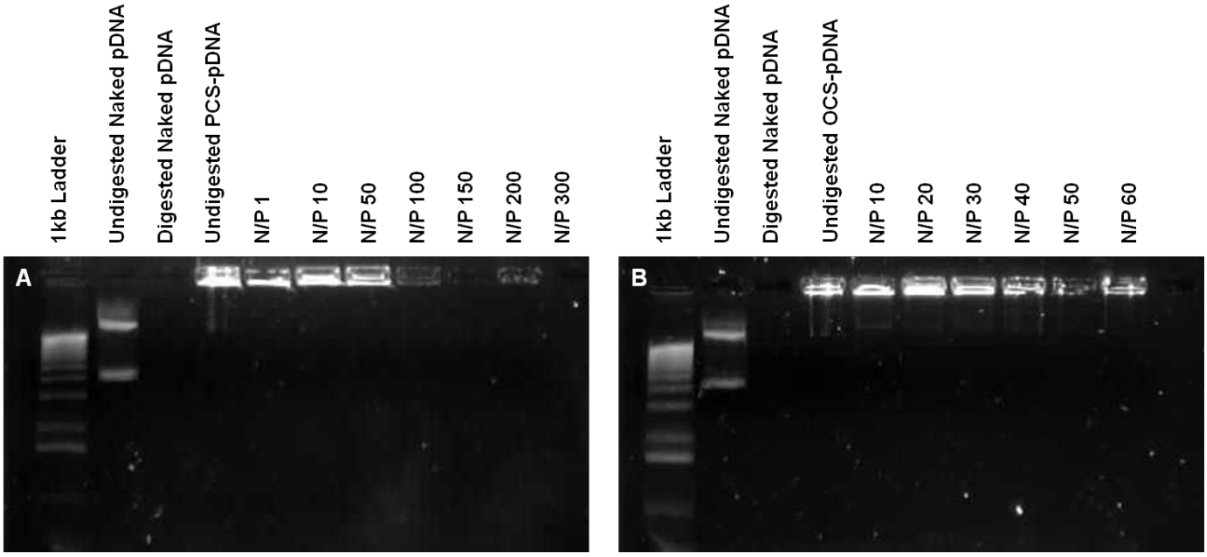

Figure 2: Effect of MW and N/P ratio on chitosan-pDNA nanoparticle stability. A DNase I degradation assay run on a 1% agarose gel. (A) shows PCS-pDNA nanoparticles at N/P 1-300 along with a 1kb ladder, undigested naked pDNA, digested naked pDNA and undigested PCS-pDNA nanoparticles (N/P 150). (B) shows the OCS-pDNA nanoparticles at N/P 10-60 along with a 1kb ladder, undigested naked pDNA, digested naked pDNA and undigested OCS-pDNA nanoparticles (N/P 20). DNase I cause degradation of naked pDNA while pDNA complexed with chitosan is protected from degradation and retained in the well – an indication of stability.

3.2 Development of an MSC transfection protocol using chitosan-pDNA nanoparticles

3.2.1 Effect of MW, N/P ratio and pDNA dose on MSC transgene expression

The results shown in Figure 3A clearly demonstrate that N/P 10 is the optimal N/P ratio for PCS-pDNA nanoparticles as it leads to significantly higher luciferase expression compared to N/P 50, 100 and 150 at days 7, 10 and 14 with peak expression occurring at day 10 post-transfection (6 X 10^5 RLU). Conversely, N/P 20 is the optimal N/P ratio for OCS-pDNA nanoparticles as it leads to significantly higher luciferase expression compared to other N/P ratios at days 10 and 14 (6 X 10^5 RLU) (Figure 3B). PCS-pGLuc nanoparticles carrying a 2 or 5µg/well dose achieved the highest levels of transfection producing a peak luciferase expression of 6X10^5 RLU at day 10 (Figure 3C). The

2µg/well pDNA dose is highest at day 14 so this formulation – N/P 10 carrying 2µg of pDNA was chosen as the optimal formulation for MSC transfection. Figure 3D depicts what happens when the pDNA dose carried by OCS nanoparticles was increased from 0.33µg (manufacturers' instructions) to 0.5, 1, 2 and 5µg/well using the optimal N/P ratio (N/P 20). There was a significant increase in luciferase expression with the 2µg/well dose leading to significantly higher luciferase expression than other pDNA doses at days 10 and 14 ($1X10^7$). Taken together, the OCS group produced a two-fold higher expression level compared to PCS-pGLuc.

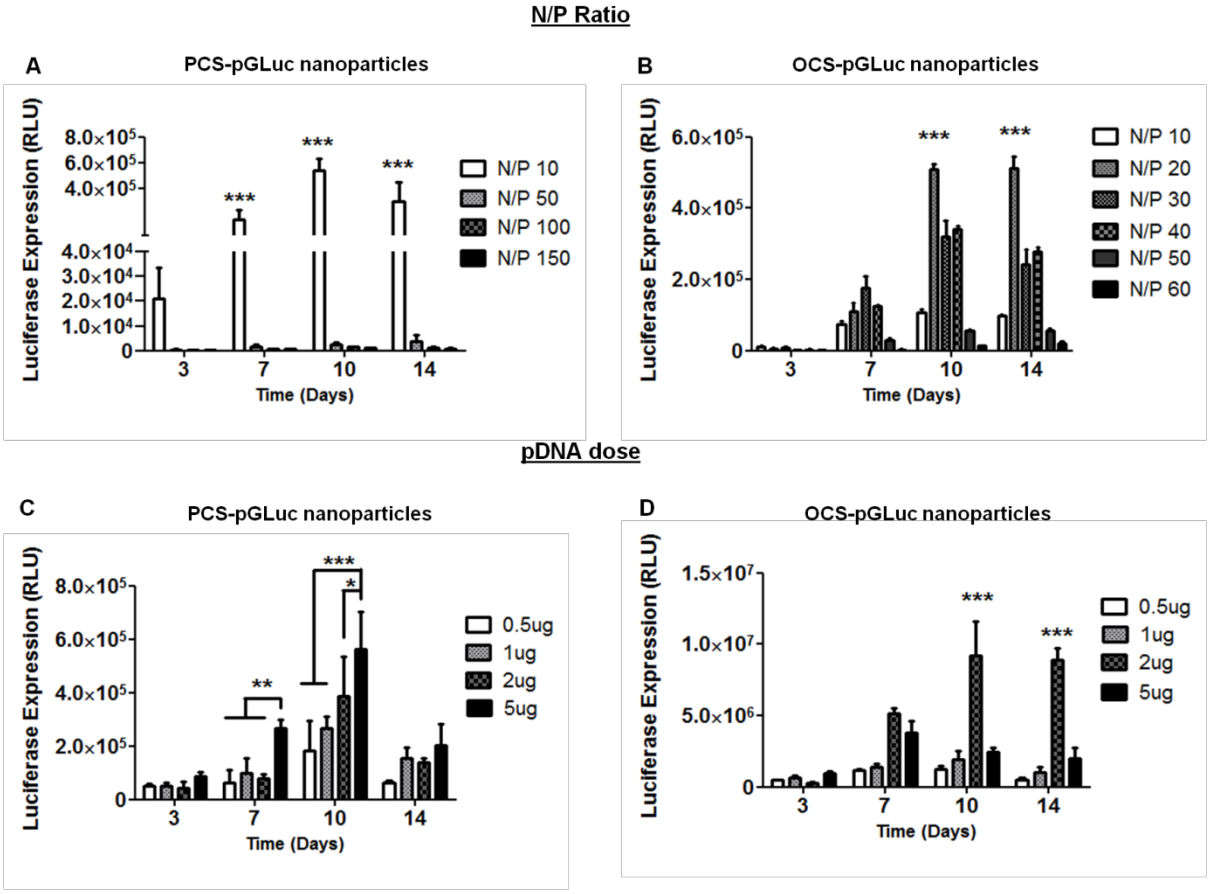

Figure 3: Effect of MW, N/P ratio and pDNA dose on MSC transgene expression. *Gaussia* Luciferase gene expression was observed over time in rMSCs transfected with PCS-pDNA (A and C) and OCS-pDNA (B and D). Nanoparticles at a range of N/P ratios (A and B) and pDNA dose (C and D) were assessed. PCS-pDNA nanoparticles formulated at N/P 10 carrying 2µg of pDNA prove to optimal for MSC transfection with luciferase expression of $6X10^5$ RLU while OCS-pDNA nanoparticle formulated at N/P 20 carrying 2µg of pDNA caused MSCs luciferase expression to reach $1X10^7$ RLU. Data plotted shows mean ± standard deviation (n=3) and * $p<0.05$, ** $p<0.01$ and *** $p<0.001$.

3.2.2 Effect of MW on MSC transfection efficiency

Luciferase expression gives an indication of overall transgene expression from the cell population but in order to definitively quantify the proportion/number of cells transfected and to visualize transfected cells, MSCs were transfected with the gene for green fluorescent protein (pGFP). PCS-pGFP and OCS-pGFP nanoparticles were produced using optimal N/P ratios (N/P 10 for PCS and N/P 20 for OCS) and pDNA doses (2µg) established from the results presented in Figure 3 and compared to PEI at N/P 7 carrying 2µg of pDNA from results established within our laboratory previously [12]. Images taken 7 days post-transfection show cells expressing GFP on their surface, indicating successful transfection (Figure 4A-C). When quantified, the transfection efficiency achieved using PCS-pGFP nanoparticles was very low at about 1.6%; however over 45% of cells transfected with OCS-pGFP are expressing GFP by day 7 and expression is sustained over 14 days (Figure 4D). When compared to the positive control, PEI led to a higher transfection initially; however, the OCS-pGFP nanoparticles cause significantly higher GFP expression by the MSCs at days 7, 10 and 14.

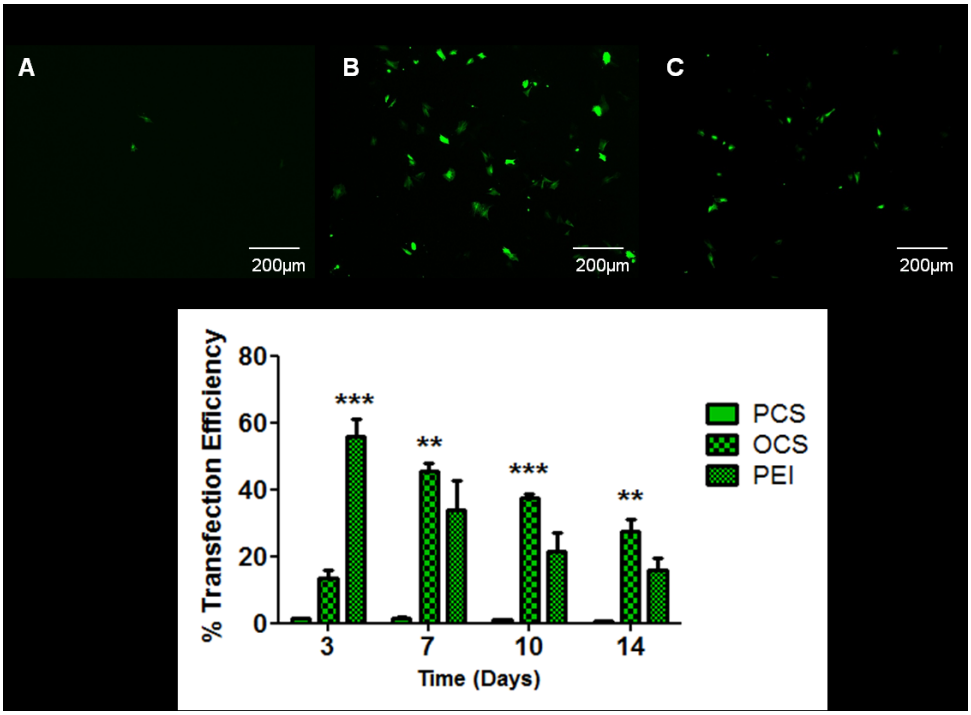

Figure 4: Effect of MW on MSC transfection efficiency. Transfection efficiency of PCS-pGFP (N/P 10, 2µg pGFP) and OCS-pGFP (N/P 20, 2µg pGFP) nanoparticles was compared using fluorescent microscopy and flow cytometry. Images A-C were taken 7 days post-transfection using a Leica Systems microscope.Green cells signify positive transfection. The percentage of cells expressing GFP was quantified using flow cytometry (D). Data plotted shows mean ± standard deviation (n=3), ** $p<0.01$ and *** $p<0.001$.

3.2.3 Assessment of chitosan-pDNA nanoparticle toxicity

As well as efficiently transfecting cells, an essential characteristic of a successful gene delivery vector is biocompatibility. While chitosan is considered to be relatively non-toxic, the PCS-pDNA and OCS-pDNA nanoparticles used in this study had an overall cationic surface charge at the N/P ratios used for transfection which may have an adverse effect on cell viability. To investigate this, an MTT assay was carried out. The effect of the PCS-pDNA and OCS-pDNA nanoparticles on MSCs at 1, 3 and 7 days post-transfection was compared to the cytotoxic effects of PEI-pDNA nanoparticles, a non-viral gene delivery vector gold standard. The results demonstrated that neither of the chitosan vectors are cytotoxic as neither PCS nor OCS-pDNA nanoparticles caused a drop in cell viability up to 7 days post-transfection (Figure 5A). Conversely, the MSCs transfected using PEI-pDNA nanoparticles suffer a 40% loss in cell number over 7 days. This result reiterates previous studies on chitosan which show that it is biocompatible causing negligible cytotoxicity [14].

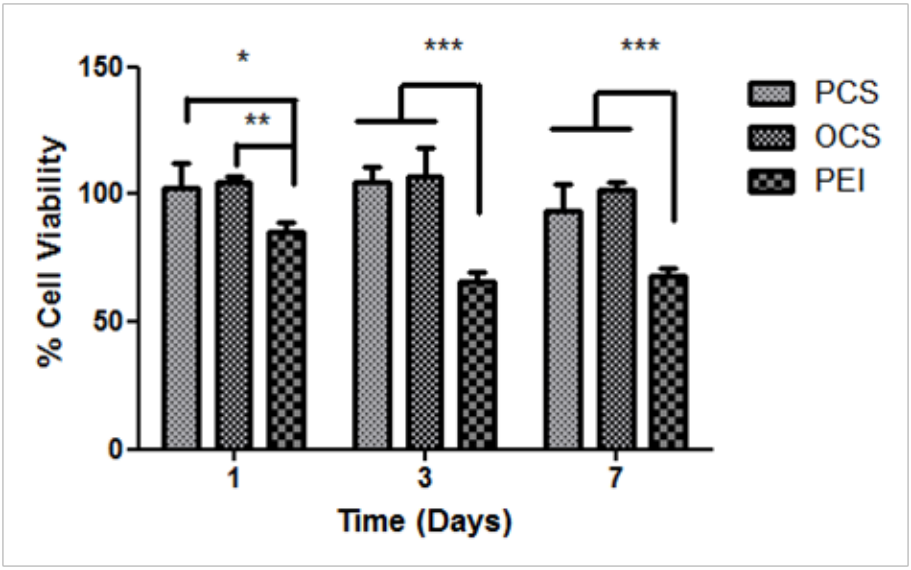

Figure 5: Assessment of cell viability post transfection. MSCs were transfected with PCS-pDNA (N/P 10, 5µg pDNA) and OCS-pDNA (N/P 20, 2µg DNA) nanoparticles and cell viability was assessed 1, 3 and 7 days post-transfection using MTT metabolic activity assay. Results were compared to PEI-pDNA (N/P 7, 2µg pDNA) transfected cells and untransfected cells served as a 100% control. Neither chitosan vector was cytotoxic while PEI causes a 40% reduction in cell viability. Data plotted shows mean ± standard deviation (n=3) and * $p<0.05$, ** $p<0.01$ and *** $p<0.001$.

3.3 Incorporation of chitosan-pDNA nanoparticles into collagen-based scaffolds to produce gene-activated scaffolds

The scaffolds used in this study include a collagen scaffold and collagen-hydroxyapatite (CHA) scaffold for bone repair, and a collagen-hyaluronic acid (CHyA) with properties optimised for cartilage regeneration [29, 36]. The optimised PCS- and OCS-pDNA nanoparticles from the previous experiments were soak-loaded onto each scaffold and the effect of the composition of each scaffold on transfection efficiency was monitored.

3.3.1 Assessment of gene-activated scaffold architecture

Analysis following loading revealed that the PCS-pDNA nanoparticles are evenly distributed throughout the scaffold but appear to be embedded in the scaffold struts in the CHyA scaffold suggesting that the nanoparticles are tightly bound to the scaffold (Figure 6A). Conversely, the OCS-pDNA nanoparticles appear to be more evenly distributed throughout the each scaffold with more limited evidence of embedding within the scaffold structure (Figure 6B).

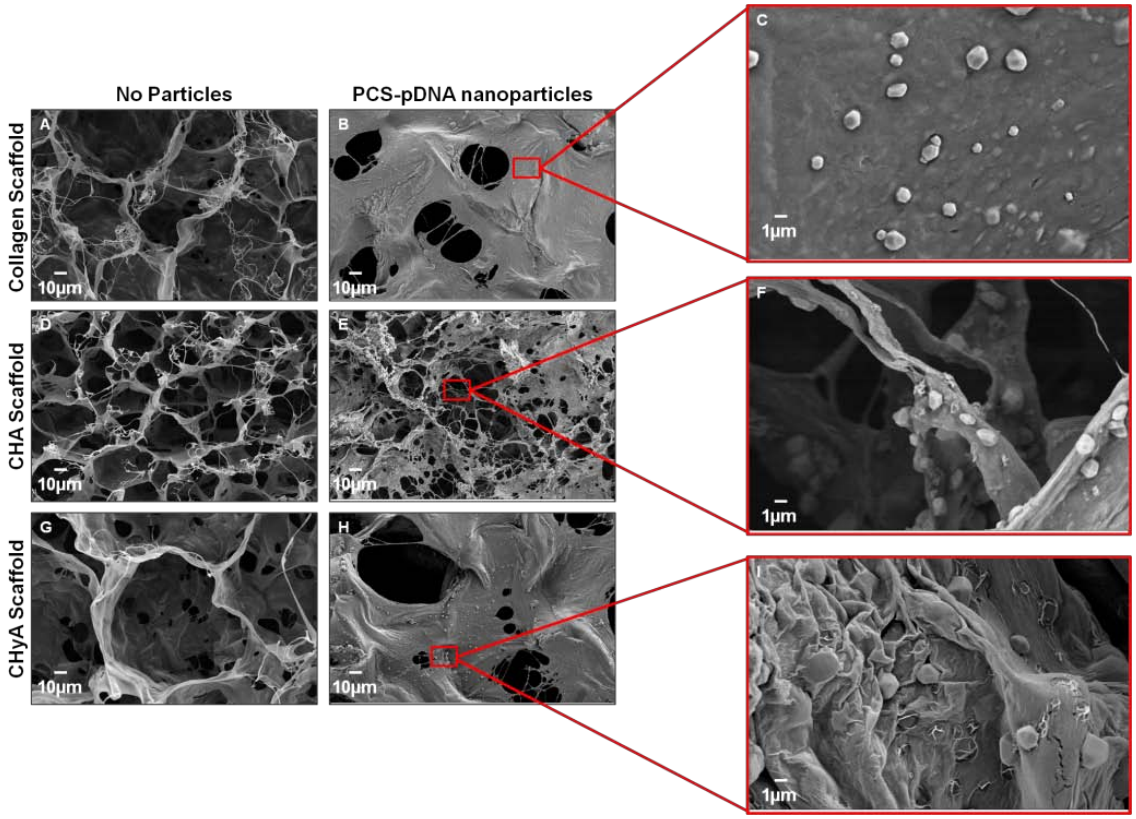

Figure 6A: Assessment of PCS-pDNA-activated scaffold architecture. PCS-pDNA nanoparticles were incorporated into three scaffolds; collagen alone (A-C), CHA (D-F) and CHyA (G-I) and imaged at various magnifications using scanning electron microscopy. Nanoparticles are homogenously dispersed within the pores but appear to be embedded within the CHyA matrix.

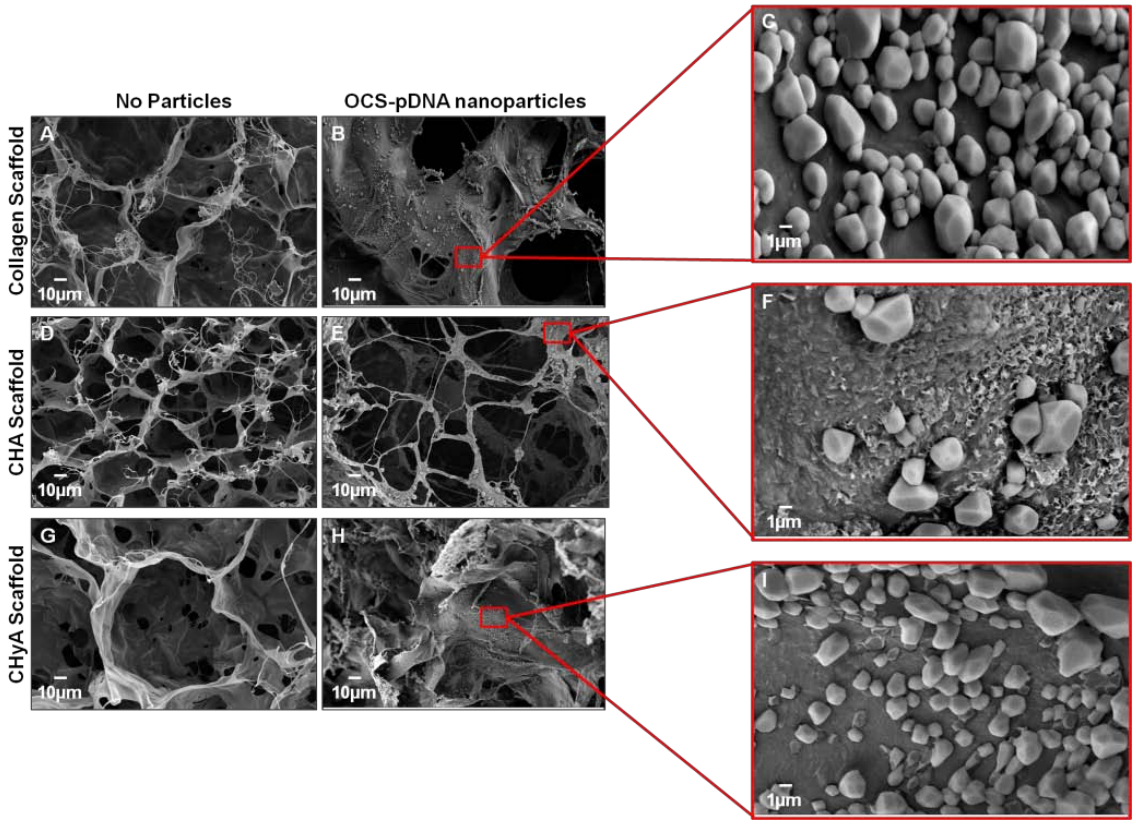

Figure 6B: Assessment of OCS-pDNA-activated scaffold architecture. OCS-pDNA nanoparticles were incorporated into three scaffolds; collagen alone (A-C), CHA (D-F) and CHyA (G-I) and imaged at various magnifications using scanning electron microscopy. Nanoparticles appear homogenously dispersed within the pores.

3.3.2 Measurement of transgene expression from MSCs seeded on gene-activated scaffolds

As N/P ratio and pDNA dose were such important factors in influencing transfection efficiency in monolayer, these experiments were initially repeated on the 3D collagen only scaffolds (PCS-pDNA nanoparticles at N/P ratios of 1-300 and OCS-pDNA nanoparticles at N/P ratios of 10-60 (results not shown)). The results informed us that transfection was very low at all N/P ratios with PCS particles and varying the pDNA dose from 0.5µg-20µg showed no improvement with luciferase levels peaking at $2.5X10^4$ RLU, a result lower than that achieved in monolayer (Figure 3C). When PCS-pDNA nanoparticles were applied to CHA and CHyA scaffolds, even lower transgene expression was recorded (Figure 7A); luciferase expression from MSCs on the CHA scaffold was just $1X10^3$ RLU while the CHyA was approximately $1X10^4$ RLU. The reason for this decrease in transfection efficiency between 2D and 3D systems may be due to interactions between PCS and collagen in the scaffold

preventing uptake of PCS-pDNA nanoparticles by the cells as was indicated in the SEM images (Figure 6A).

In contrast, OCS-pDNA nanoparticles performed as positively on 3D collagen scaffolds, as they had in monolayer culture. Preliminary transfection studies testing N/P ratios (10-60) and pDNA dose (0.5-20µg/scaffold) (results not shown) indicated that nanoparticles formulated at N/P 20 carrying a pDNA dose of 2µg resulted in the highest levels of transgene expression. When compared to the CHA and CHyA (Figure 7B), gene expression from the cells was initially significantly higher on the collagen only gene-activated scaffold, but interestingly, gene expression from the CHyA scaffold peaks later, at day 21, becoming significantly higher than collagen alone and CHA at the later time-points.

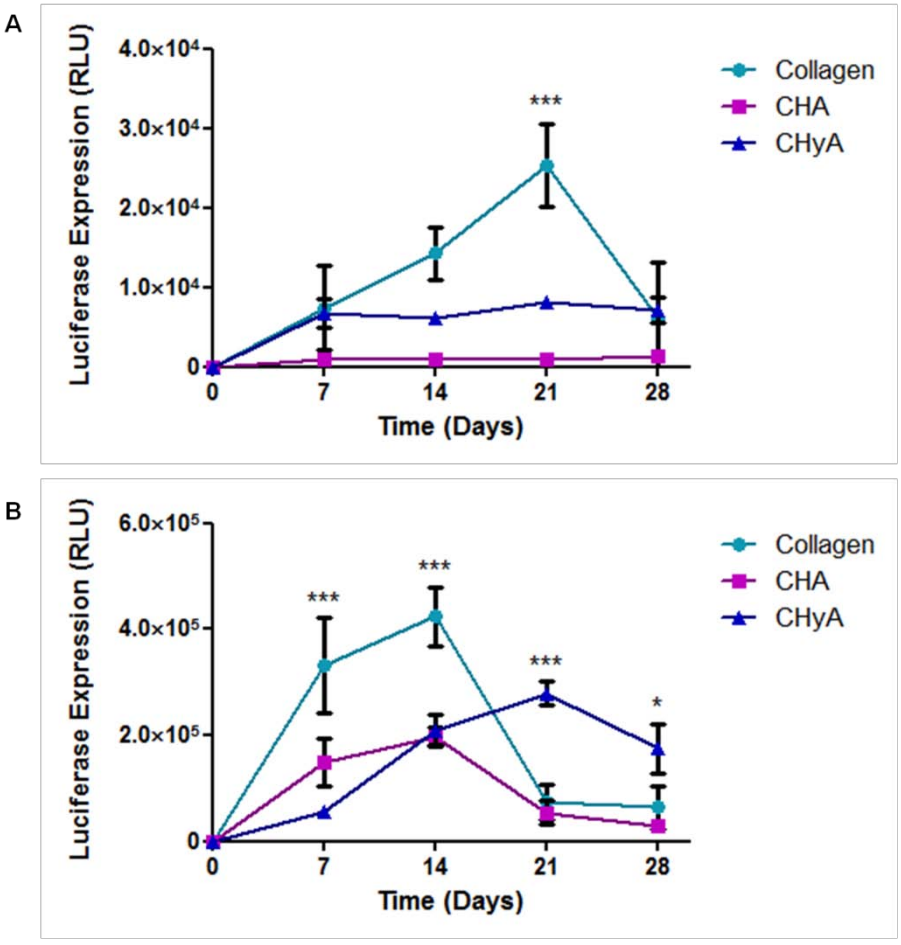

Figure 7: Measurement of transgene expression from MSCs seeded on gene-activated scaffolds. Relative *Gaussia* Luciferase gene expression was monitored over time from MSCs transfected with PCS-pGLuc at N/P 10 carrying 2µg pGLuc (A) and OCS-pGLuc at N/P 20 carrying 2µg pGLuc (B) incorporated into three scaffolds of different composition; collagen, CHA and CHyA. OCS-pGLuc nanoparticles produce higher levels of luciferase than PCS-pGLuc nanoparticles and transgene expression varies with scaffold composition. Data plotted shows mean ± standard deviation (n=3) and * $p<0.05$, ** $p<0.01$ and *** $p<0.001$.

4. Discussion

The objective of this study was firstly to develop methodology for formulating chitosan-pDNA nanoparticles with properties suitable for efficient MSC transfection, and secondly, to create a series of gene-activated scaffolds by incorporating the optimised chitosan-pDNA nanoparticles into collagen-based scaffolds with properties previously optimized for tissue regeneration. The MW of chitosan proved to be important in the nanoparticle formulation process as was the N/P ratio which influenced nanoparticle size, zeta potential, encapsulation efficiency and ultimately, transfection efficiency. A transfection efficiency greater than 45% was achieved in MSCs in monolayer culture using oligochitosan-pDNA nanoparticles and this level of efficiency was translated to 3D experiments when the nanoparticles were incorporated into three types of collagen-based scaffold; collagen alone, collagen hydroxyapatite (CHA) and collagen hyaluronic acid (CHyA). Interestingly, the kinetics of gene expression varied significantly between scaffolds of different composition. Therefore, this work allowed for the development of a range of biocompatible platforms that can be functionalised for gene delivery in which a sustained but ultimately transient gene expression profile was obtained while still achieving transfection efficiencies in stem cells sufficient to elicit a therapeutic response [30].

There is currently no ideal non-viral gene delivery vector. ‘Gold standard’ vectors include Lipofectamine 2000™ and polyethyleneimine (PEI) which can achieve high transfection efficiencies in many cell types, but can also cause cytotoxicity [14, 15, 44]. Chitosanis known to be non-toxic and good transfection efficiency has been reported in some cell lines [16, 25, 26, 45]. However, in this study, the cell type of interest was the mesenchymal stem cell (MSCs), a cell type of greater clinical significance in tissue engineering applications due to its ability to differentiate into a number of mesoderm-derived cell types, but which is notoriously difficult to transfect [46]. Very little work has been done on chitosan mediated transfection of MSCs with the highest transfection efficiency reported was 18% with a medium molecular weight (MW) chitosan [21]. Recent studies indicate that low MW, highly deacetylated oligomeric chitosan can achieve >60% transfection efficiency in HEK293 cells [26] and has been used in vivo in corneal [31] and retinal gene delivery [32]. It is clear therefore that molecular weight (MW) and degree of deacetylation (DD) have a major influence on transfection efficiency and in this study we sought to compare medium MW polymeric chitosan (PCS) with low MW

oligomeric chitosan (OCS) and optimize a transfection protocol specifically for use on MSCs, a more clinically relevant cell type for orthopedic tissue engineering, than investigated previously.

It is hypothesized that chitosan-based gene delivery vectors enter cells via charge-mediated endocytosis [47], therefore, chitosan-pDNA nanoparticles need to be positively charged to bind to the negatively charged cell membrane, and have a diameter of <200nm to enable endocytosis [43]. AFM images revealed that polymeric chitosan (PCS)-pDNA nanoparticles appear homogenous in size with an average diameter of ~190 nm while oligomeric chitosan- (OCS)-pDNA nanoparticles have a less defined shape and a smaller diameter of ~120 nm. The difference in morphology is likely due to the use of a cross-linker (sodium tripolyphosphate (TPP)) in the formulation on PCS-pDNA nanoparticles which causes a controlled ionotropic gelation of the nanoparticles [19, 48]. Without TPP PCS-pDNA nanoparticles were in the micron size range and therefore unsuitable for gene delivery [43, 47]. TPP did not cause changes in size in the formulation of OCS-pDNA nanoparticles and thus was not used which explains their irregular shape. This size analysis was supported with dynamic light scattering experiments where N/P ratios of 10-150 in the PCS group and all N/P ratios (10-60) in the OCS group were <200nm. The zeta potential (ZP) of the nanoparticles is governed by the amount of cationic material (chitosan) in the particle which explains why at N/P 1, PCS-pDNA nanoparticles carried a negative zeta potential, indicating that there was too little chitosan to fully complex with the pDNA. Complexation efficiency is also lowest at N/P 1 confirming this statement

Chitosan was able to protect pDNA from DNase I degradation which may indicate nanoparticle stability in physiological conditions. There appears to be less pDNA fluorescence at higher N/P ratios in the PCS-pDNA group which is most likely due to over encapsulation of pDNA by excess PCS. OCS had greater complexation efficiency for pDNA than PCS (>90% compared to an average of 80% for PCS-pDNA), however, pDNA appears to be released from OCS faster than from PCS as evidenced by gel electrophoresis studies where there is evidence of faint bands seen at all N/P ratios, but more so at lower N/P ratios, suggesting that the pDNA is beginning to be released from the OCS. This result is in agreement with other reports which state that low MW chitosan forms less stable nanoparticles with pDNA than with high MW [23, 25, 49, 50]. While stability is important extracellularly, release of the pDNA is critical in ensuring transfection so OCS-pDNA nanoparticles formulated at all the N/P ratios investigated were deemed suitable for transfection experiments.

In the development of a transfection protocol, the N/P ratio proved to have a major impact on transgene expression by the cells with N/P 10 (PCS) and N/P 20 (OCS) transfected cells producing significantly higher amounts of luciferase than the other N/P ratios. Neither of the papers describing chitosan vectors for gene delivery to MSCs tested different N/P ratios [15, 21], however on HEK293 cells transfection efficiency was highest at N/P 10 [51]. When OCS-pDNA nanoparticles were used to transfect HEK293 cells, luciferase expression increased along with increasing N/P ratio (10 up to 60) [25], while in this study, N/P 20, 30 and 40 led to higher transfection efficiencies than other N/P ratios showing differences in transfection efficiencies between different cell types. The pDNA dose also has a significant influence on chitosan-pDNA nanoparticle transfection efficiency with the 2µg pDNA dose causing the highest levels of luciferase expression while higher doses resulted in no increase or a reduction in transgene expression. This is a well documented phenomenon; one laboratory reported that increasing the dose of pDNA from 0.5µg-2.5µg/well increased transfection efficiency but any higher doses led to reduced transgene expression [52]. Overall, the best PCS-pDNA nanoparticle formulation had a transfection efficiency of just 1.6%. This result is in line with what has previously been published on using chitosan for gene delivery to MSCs [15]. On the other hand, the transfection efficiency achieved with the optimised OCS-pDNA nanoparticles led to a 45% transfection efficiency which was sustained over the course of the experiment. This is an excellent result as it has been shown that sustained expression of therapeutics over time at a defect site can enhance tissue healing when compared to defects treated with burst release of proteins or drugs [53]. A transfection efficiency of 45% efficiency is also comparable to that seen for PEI which is a gold standard non-viral vector [54] and this study represents the first time that a chitosan-based gene delivery system has caused comparable transfection efficiencies to PEI in MSCs.

The reason behind the different transfection efficiencies seen with PCS and OCS may be explained by the mechanism of cell entry utilised by each vector. It has been shown that PCS-pDNA nanoparticles enter cells predominantly through the clathrin-mediated endocytosis pathway which carries cargo through the cytoplasm in acidic endosomes [47]. It is thought that polymers that are capable of buffering this acidic environment can cause an increase in osmotic pressure and rupture the endosome, liberating the delivery vector and its gene cargo. PEI is a delivery vector known to act

in this way through what is termed the ‘proton sponge’ effect [11, 55]. However, the inability of PCS to act like a proton sponge may explain the low transfection efficiency achieved with this polymer in this and other studies [15, 21, 56]. Interestingly, OCS-pDNA nanoparticles are reported to enter cells *via* clathrin-independent pathways, namely the caveolae route of endocytosis. Much less is known about this route of entry but a different entry mechanism may explain the difference in transfection efficiency seen by the two types of chitosan [47].

Even though chitosan is a biocompatible material, there has been some suggestion that cationic nanoparticles, such as the ones used in this study can be cytotoxic. Neither of the optimised formulations of chitosan nanoparticles tested caused a decrease in cell viability at any time-point up to 7 days post transfection. On the other hand, PEI-pDNA polyplexes caused a 40% drop in cell viability 3 days post-transfection. This result is in agreement with previously published reports a dose of just 20 µg/mL of PEI was enough to cause cytotoxicity whereas 630 µg/mL of chitosan was required to induce a cytotoxic response [14, 57]. OCS has been investigated in a number of studies and has been shown to be even less cytotoxic than PCS [58-60].

Bonadio *et al.* was the first to describe the use of gene-activated matrices (GAM) for tissue engineering applications where a gene encoding a fragment of human parathyroid hormone (hPTH 1-34) in a collagen scaffold was used to treat a 1cm bone defect in a canine model [27]. Union of the bone was seen after 8 weeks and a very high 1mg dose of pDNA was required per GAM (compared to 2µg in this study) to achieve an estimated transfection efficiency of 30% (determined by RTPCR). To overcome this low efficiency, gene delivery vectors may be used; work within our group has shown that nanohydroxyapatite (nHA) particles are efficient gene delivery vectors and contribute to enhanced calcium deposition both in 2D monolayer of MSCs and 3D collagen-based scaffolds [61]. Also within our group, PEI-pDNA polyplexes have been incorporated into a series of collagen based scaffolds to create a gene-activated scaffolds for bone regeneration [12] and the combination of both nHA and PEI for independent delivery of BMP-2 and VEGF respectively, can significantly enhance bone healing with complete bridging of a critical sized defect within 4 weeks [30]. In this study, transgene expression from MSCs on the OCS-pDNA activated scaffolds is comparable to what was

reported in the PEI-pDNA study described above which indicates that this system also has potential for bone healing while avoiding the cytotoxicity associated with PEI [12, 30].

OCS-pDNA nanoparticles caused significantly higher transgene expression than PCS-pDNA regardless of scaffold material; however, scaffold composition influenced transgene expression by MSCs with the lowest luciferase expression occurring from cells on the collagen hydroxyapatite scaffold. As transgene expression on the collagen scaffold was much higher, the hydrogen bonds forming between chitosan nanoparticles and the hydroxyapatite may reduce cell uptake of the nanoparticles [62]. Furthermore, prolonged expression of luciferase is seen in the collagen hyaluronic acid scaffold where luciferase expression peaked later than the collagen alone scaffold and was higher at day 28. This may be due to an electrostatic interaction between the free amine groups on the OCS-pDNA nanoparticles and the carboxylate and/or sulphate groups on hyaluronic acid causing a delayed uptake of the nanoparticles by the MSCs.

5. Conclusion

The objectives of this study was firstly, to develop chitosan-based nanoparticles with properties that facilitate MSC transfection and secondly, to create a series of gene-activated scaffolds by incorporating the optimised chitosan-pDNA nanoparticles into collagen-based scaffolds. Following a rigorous characterisation of both PCS-pDNA and OCS-pDNA nanoparticles, the optimal formulation was found to be OCS-pDNA nanoparticles at an N/P ratio of 20 carrying 2µg of pDNA. This formulation produced a transfection efficiency of 45% in MSCs in monolayer without causing any cytotoxicity. Upon incorporation into a series of MSC seeded collagen-based scaffolds, gene expression from MSCs was highest on the collagen only scaffold but high levels of luciferase was also expressed for longer by cells on the collagen hyaluronic acid scaffold. This study has led to the development of a platform system capable of gene delivery to MSCs. The scaffolds that were functionalised in this study have already been optimised for bone and cartilage tissue engineering so the next step is to deliver osteogenic or chondrogenic genes and assessing if this gene-activated scaffold platform can further enhance bone and cartilage repair. By simply varying the scaffold composition and the gene (or combinations thereof) chosen, the system has potential for a myriad of therapeutic applications.

Acknowledgements

This work was funded by Science Foundation Ireland (SFI) Research Frontiers Programme (Grant No. 11/RFP/ENM/3053), Collagen materials were provided by Integra Life Sciences, Inc. through a Material Transfer Agreement. We also thank Dr. M. Sawkins and the **C**entre for **R**esearch on **A**daptive **N**anostructures and **N**anodevices (CRANN), Trinity College Dublin, for help with SEM and AFM imaging.

References

1. De la Riva, B., et al., *Local controlled release of VEGF and PDGF from a combined brushite–chitosan system enhances bone regeneration.* Journal of Controlled Release, 2010. **143**(1): p. 45-52.
2. Quinlan, E., et al., *Development of collagen–hydroxyapatite scaffolds incorporating PLGA and alginate microparticles for the controlled delivery of rhBMP-2 for bone tissue engineering.* Journal of Controlled Release, 2015. **198**(0): p. 71-79.
3. Khan, S.N. and J.M. Lane, *The use of recombinant human bone morphogenetic protein-2 (rhBMP-2) in orthopaedic applications.* Expert Opinion on Biological Therapy, 2004. **4**(5): p. 741-748.
4. Miyazaki, M., et al., *An update on bone substitutes for spinal fusion.* European Spine Journal, 2009. **18**(6): p. 783-799.
5. Hacein-Bey-Abina, S., et al., *Sustained Correction of X-Linked Severe Combined Immunodeficiency by ex Vivo Gene Therapy.* New england journal of medicine, 2002. **346**(16): p. 1185-1193.
6. Lee, R.J., et al., *VEGF gene delivery to myocardium deleterious effects of unregulated expression.* Circulation, 2000. **102**(8): p. 898-901.
7. Lundstrom, K. and T. Boulikas, *Viral and non-viral vectors in gene therapy: technology development and clinical trials.* Technology in cancer research & treatment, 2003. **2**(5): p. 471-486.
8. Djurovic, S., et al., *Comparison of nonviral transfection and adeno-associated viral transduction on cardiomyocytes.* Molecular biotechnology, 2004. **28**(1): p. 21-31.
9. Kay, M.A., *State-of-the-art gene-based therapies: the road ahead.* Nature Reviews Genetics, 2011. **12**(5): p. 316-328.
10. Pack, D.W., et al., *Design and development of polymers for gene delivery.* Nature Reviews Drug Discovery, 2005. **4**(7): p. 581-593.
11. Akinc, A., et al., *Exploring polyethylenimine-mediated DNA transfection and the proton sponge hypothesis.* The Journal of Gene Medicine, 2005. **7**(5): p. 657-663.
12. Tierney, E.G., et al., *The development of non-viral gene-activated matrices for bone regeneration using polyethyleneimine (PEI) and collagen-based scaffolds.* Journal of Controlled Release, 2012. **158**(2): p. 304-311.
13. Boussif, O., et al., *A versatile vector for gene and oligonucleotide transfer into cells in culture and in vivo: polyethylenimine.* Proceedings of the National Academy of Sciences, 1995. **92**(16): p. 7297-7301.
14. Regnström, K., et al., *Gene expression profiles in mouse lung tissue after administration of two cationic polymers used for nonviral gene delivery.* Pharmaceutical research, 2006. **23**(3): p. 475-482.

15. Corsi, K., et al., *Mesenchymal stem cells, MG63 and HEK293 transfection using chitosan-DNA nanoparticles.* Biomaterials, 2003. **24**(7): p. 1255-1264.
16. MacLaughlin, F.C., et al., *Chitosan and depolymerized chitosan oligomers as condensing carriers for in vivo plasmid delivery.* Journal of Controlled Release, 1998. **56**(1): p. 259-272.
17. Mao, H.-Q., et al., *Chitosan-DNA nanoparticles as gene carriers: synthesis, characterization and transfection efficiency.* Journal of Controlled Release, 2001. **70**(3): p. 399-421.
18. Ishii, T., Y. Okahata, and T. Sato, *Mechanism of cell transfection with plasmid/chitosan complexes.* Biochimica et Biophysica Acta (BBA)-Biomembranes, 2001. **1514**(1): p. 51-64.
19. Csaba, N., M. Köping-Höggård, and M.J. Alonso, *Ionically crosslinked chitosan/tripolyphosphate nanoparticles for oligonucleotide and plasmid DNA delivery.* International journal of pharmaceutics, 2009. **382**(1): p. 205-214.
20. Mumper, R.J., et al., *Novel polymeric condensing carriers for gene delivery.* Proceedings of the International Symposium on Controlled Release Bioactive Materials, 1995. **22**: p. 178-179.
21. Malakooty Poor, E., et al., *Chitosan–pDNA nanoparticle characteristics determine the transfection efficacy of gene delivery to human mesenchymal stem cells.* Artificial Cells, Nanomedicine, and Biotechnology, 2013. **1**(1): p. 1-9.
22. Mansouri, S., et al., *Chitosan-DNA nanoparticles as non-viral vectors in gene therapy: strategies to improve transfection efficacy.* European Journal of Pharmaceutics and Biopharmaceutics, 2004. **57**(1): p. 1-8.
23. Huang, M., et al., *Transfection efficiency of chitosan vectors: Effect of polymer molecular weight and degree of deacetylation.* Journal of Controlled Release, 2005. **106**(3): p. 391-406.
24. Kiang, T., et al., *The effect of the degree of chitosan deacetylation on the efficiency of gene transfection.* Biomaterials, 2004. **25**(22): p. 5293-5301.
25. Köping-Höggård, M., et al., *Improved chitosan-mediated gene delivery based on easily dissociated chitosan polyplexes of highly defined chitosan oligomers.* Gene Ther, 2004. **11**(19): p. 1441-1452.
26. Strand, S.P., et al., *Molecular design of chitosan gene delivery systems with an optimized balance between polyplex stability and polyplex unpacking.* Biomaterials, 2010. **31**(5): p. 975-987.
27. Bonadio, J., et al., *Localized, direct plasmid gene delivery in vivo: prolonged therapy results in reproducible tissue regeneration.* Nature medicine, 1999. **5**(7): p. 753-759.
28. O'Brien, F.J., J.P. Gleeson, and N. Plunkett, *Collagen/hydroxyapatite composite scaffold, and process for the production thereof*. 2013, Google Patents.
29. Levingstone, T.J., et al., *A biomimetic multi-layered collagen-based scaffold for osteochondral repair.* Acta Biomaterialia, 2014. **10**(5): p. 1996-2004.
30. Curtin, C.M., et al., *Combinatorial Gene Therapy Accelerates Bone Regeneration: Non-Viral Dual Delivery of VEGF and BMP2 in a Collagen-Nanohydroxyapatite Scaffold.* Advanced Healthcare Materials, 2014.
31. Klausner, E.A., et al., *Ultrapure chitosan oligomers as carriers for corneal gene transfer.* Biomaterials, 2010. **31**(7): p. 1814-1820.
32. Puras, G., et al., *Low molecular weight oligochitosans for non-viral retinal gene therapy.* European Journal of Pharmaceutics and Biopharmaceutics, 2013. **83**(2): p. 131-140.
33. O'Brien, F.J., et al., *Influence of freezing rate on pore structure in freeze-dried collagen-GAG scaffolds.* Biomaterials, 2004. **25**(6): p. 1077-1086.
34. O'Brien, F.J., et al., *The effect of pore size on cell adhesion in collagen-GAG scaffolds.* Biomaterials, 2005. **26**(4): p. 433-441.
35. Gleeson, J., N. Plunkett, and F. O'Brien, *Addition of hydroxyapatite improves stiffness, interconnectivity and osteogenic potential of a highly porous collagen-based scaffold for bone tissue regeneration.* Eur Cell Mater, 2010. **20**: p. 218-230.

36. Matsiko, A., et al., *Addition of hyaluronic acid improves cellular infiltration and promotes early-stage chondrogenesis in a collagen-based scaffold for cartilage tissue engineering.* Journal of the Mechanical Behavior of Biomedical Materials, 2012. **11**: p. 41-52.
37. Sambrook, J., E.F. Fritsch, and T. Maniatis, *Molecular cloning: a laboratory manual.* Cold Spring Harbor Laboratory Press, New York, 1989. **6.15**: p. 6-44.
38. Lepecq, J.B. and C. Paoletti, *A fluorescent complex between ethidium bromide and nucleic acids: Physical—Chemical characterization.* Journal of Molecular Biology, 1967. **27**(1): p. 87-106.
39. O'Brien, F.J., et al., *Influence of freezing rate on pore structure in freeze-dried collagen-GAG scaffolds.* Biomaterials, 2004. **25**(6): p. 1077-1086.
40. Haugh, M.G., C.M. Murphy, and F.J. O'Brien, *Novel Freeze-Drying Methods to Produce a Range of Collagen-Glycosaminoglycan Scaffolds with Tailored Mean Pore Sizes.* Tissue Engineering Part C-Methods, 2010. **16**(5): p. 887-894.
41. Haugh, M.G., M.J. Jaasma, and F.J. O'Brien, *The effect of dehydrothermal treatment on the mechanical and structural properties of collagen-GAG scaffolds.* Journal of Biomedical Materials Research Part A, 2009. **89**(2): p. 363-369.
42. Oh, N. and J.-H. Park, *Endocytosis and exocytosis of nanoparticles in mammalian cells.* International journal of nanomedicine, 2014. **9**(Suppl 1): p. 51-63.
43. Rejman, J., et al., *Size-dependent internalization of particles via the pathways of clathrin-and caveolae-mediated endocytosis.* Biochem. J, 2004. **377**: p. 159-169.
44. Agirre, M., et al., *Low Molecular Weight Chitosan (LMWC)-based Polyplexes for pDNA Delivery: From Bench to Bedside.* Polymers, 2014. **6**(6): p. 1727-1755.
45. Sato, T., T. Ishii, and Y. Okahata, *In vitro gene delivery mediated by chitosan. Effect of pH, serum, and molecular mass of chitosan on the transfection efficiency.* Biomaterials, 2001. **22**(15): p. 2075-2080.
46. Hamm, A., et al., *Efficient transfection method for primary cells.* Tissue Eng, 2002. **8**(2): p. 235-45.
47. Garaiova, Z., et al., *Cellular uptake of DNA–chitosan nanoparticles: The role of clathrin-and caveolae-mediated pathways.* International Journal of Biological Macromolecules, 2012. **51**(5): p. 1043-1051.
48. Calvo, P., et al., *Novel hydrophilic chitosan-polyethylene oxide nanoparticles as protein carriers.* Journal of Applied Polymer Science, 1997. **63**(1): p. 125-132.
49. Köping-Höggård, M., et al., *Relationship between the physical shape and the efficiency of oligomeric chitosan as a gene delivery system in vitro and in vivo.* The Journal of Gene Medicine, 2003. **5**(2): p. 130-141.
50. Strand, S.P., et al., *Influence of chitosan structure on the formation and stability of DNA-chitosan polyelectrolyte complexes.* Biomacromolecules, 2005. **6**(6): p. 3357-3366.
51. Lavertu, M., et al., *High efficiency gene transfer using chitosan/DNA nanoparticles with specific combinations of molecular weight and degree of deacetylation.* Biomaterials, 2006. **27**(27): p. 4815-4824.
52. Romøren, K., et al., *The influence of formulation variables on in vitro transfection efficiency and physicochemical properties of chitosan-based polyplexes.* International journal of pharmaceutics, 2003. **261**(1): p. 115-127.
53. Jeon, O., et al., *Long-term delivery enhances in vivo osteogenic efficacy of bone morphogenetic protein-2 compared to short-term delivery.* Biochemical and biophysical research communications, 2008. **369**(2): p. 774-780.
54. Schaffert, D. and E. Wagner, *Gene therapy progress and prospects: synthetic polymer-based systems.* Gene Ther, 2008. **15**(16): p. 1131-1138.
55. Behr, J.-P., *The proton sponge: a trick to enter cells the viruses did not exploit.* CHIMIA International Journal for Chemistry, 1997. **51**(1-2): p. 34-36.

56. Moreira, C., et al., *Improving chitosan-mediated gene transfer by the introduction of intracellular buffering moieties into the chitosan backbone.* Acta biomaterialia, 2009. **5**(8): p. 2995-3006.
57. Köping-Höggård, M., et al., *Chitosan as a nonviral gene delivery system. Structure–property relationships and characteristics compared with polyethylenimine in vitro and after lung administration in vivo.* Gene therapy, 2001. **8**: p. 1108-1121.
58. Thanou, M., et al., *Quaternized chitosan oligomers as novel gene delivery vectors in epithelial cell lines.* Biomaterials, 2002. **23**(1): p. 153-159.
59. Richardson, S.W., H.J. Kolbe, and R. Duncan, *Potential of low molecular mass chitosan as a DNA delivery system: biocompatibility, body distribution and ability to complex and protect DNA.* International journal of pharmaceutics, 1999. **178**(2): p. 231-243.
60. Kean, T. and M. Thanou, *Biodegradation, biodistribution and toxicity of chitosan.* Advanced Drug Delivery Reviews, 2010. **62**(1): p. 3-11.
61. Curtin, C.M., et al., *Innovative Collagen Nano-Hydroxyapatite Scaffolds Offer a Highly Efficient Non-Viral Gene Delivery Platform for Stem Cell-Mediated Bone Formation.* Advanced Materials, 2012. **24**(6): p. 749-754.
62. Xianmiao, C., et al., *Properties and in vitro biological evaluation of nano-hydroxyapatite/chitosan membranes for bone guided regeneration.* Materials Science and Engineering: C, 2009. **29**(1): p. 29-35.